

Strong decay of low-lying S_{11} and D_{13} nucleon resonances to pseudoscalar mesons and octet baryons

C. S. An^{*} and B. Saghai[†]

*Institut de Recherche sur les lois Fondamentales de l'Univers,
DSM/Irfu, CEA/Saclay, F-91191 Gif-sur-Yvette, France*

(Dated: November 19, 2018)

Abstract

Partial decay widths of lowest lying nucleon resonances $S_{11}(1535)$, $S_{11}(1650)$, $D_{13}(1520)$ and $D_{13}(1700)$ to the pseudoscalar mesons and octet baryons are studied within a chiral constituent quark model. Effects of the configurations mixing between the states $|N_8^2 P_M\rangle$ and $|N_8^4 P_M\rangle$ are considered, taking into account $SU(6) \otimes O(3)$ breaking effects. In addition, possible contributions of the strangeness components in the S_{11} resonances are investigated. Experimental data for the partial decay widths of the S_{11} and D_{13} resonances are well reproduced. Predictions for coupling constants of the four nucleon resonances to pseudoscalar mesons and octet baryons, crucial issues in the photo- and hadron-induced meson production reactions, are reported. Contributions from five-quark components in the S_{11} resonances are found crucial in reproducing the partial widths.

PACS numbers: 12.39.-x, 13.30.Eg, 14.20.Gk

^{*}chunsheng.an@cea.fr

[†]bijan.saghai@cea.fr

I. INTRODUCTION

Production of mesons with hidden or open strangeness via electromagnetic or hadronic probes, in the baryon resonance energy range, is subject to extensive experimental and theoretical investigations. In this realm, partial decay widths of resonances to meson-baryon final states, as well as the relevant coupling constants are crucial, but not well enough known [1], ingredients in our understanding of the reaction mechanisms, and also of the nature of those resonances.

Phenomenological approaches, dealing with the above ingredients, arise mainly from two families of formalisms: effective Lagrangians based on meson-baryon degrees of freedom [2–30] and QCD based/inspired models [31–46].

Among the low-lying nucleon excitations, the $S_{11}(1535)$ resonance plays a special role due to its large ηN decay width [1], though its mass is very close to the threshold of the decay. Moreover, in the KY production reactions the importance of the $S_{11}(1650)$ is well established. For the two other first orbitally excited (quark model prediction) nucleon resonances, $D_{13}(1520)$ and $D_{13}(1700)$, the couplings to the pseudoscalar meson and octet baryons seem to be rather weak, but the first one is known to intervene significantly in the polarization asymmetries.

The observables of interest in this paper are partial decay widths. Experimental values are available [1] for all four resonances' decay to πN and ηN final states, as well as for the $S_{11}(1650)$ and $D_{13}(1700)$ resonances to $K\Lambda$, though with rather large uncertainties. However, in spite of extensive studies mentioned above, to our knowledge no single formalism has reproduced *simultaneously* those partial widths. The only exception here is a very recent comprehensive study [46] based on the $1/N_C$ expansion approach. Besides the fact that a large number of investigations concentrate on the S_{11} resonances, recent copious photoproduction data have not yet been fully exploited by sophisticated coupled-channels phenomenological approaches. The main motivation of the present work is then to study those partial decay widths within a QCD inspired formalism, and shed light on the structure of those baryons.

The theoretical frame of the present work is based on a chiral constituent quark model (χ CQM), complemented with the $SU(6) \otimes O(3)$ symmetry breaking effects. The outcomes of those formalisms are compared to the known [1] partial decay widths of the above mentioned

resonances. This approach gives satisfactory results for the D_{13} resonances, but misses partly the data for S_{11} .

Attempting to cure the observed theory / experiment discrepancies, the χ CQM is subsequently complemented with including contributions from higher Fock-components, namely, five-quark configurations. Actually, several authors [47–54], have shown that contributions from the five-quark components are quite significant in describing the properties of baryons and their electromagnetic and strong decays, especially contributions from the $qqqq\bar{q} \rightarrow M(\gamma) + qqq$ transitions. For recent reviews on five-quark components in baryons, see Refs. [55–57].

The extended χ CQM allows reproducing the known partial decay widths for both S_{11} resonances. Following the successful results obtained for low-lying baryon resonances, we put forward predictions for the coupling constants of those resonances to seven meson-baryon final states, i.e. $\pi^0 p$, $\pi^+ n$, ηp , $K^+ \Lambda$, $K^0 \Sigma^+$, $K^+ \Sigma^0$, $\eta' p$.

The present manuscript is organized in the following way: in section II, we present the theoretical formalism which includes the wave functions, strong decays and the resulting transition amplitudes for the $S_{11}(1535)$, $S_{11}(1650)$, $D_{13}(1520)$ and $D_{13}(1700)$ to the pseudoscalar mesons and octet baryons. Numerical results are given in section III, and finally section IV contains summary and conclusions.

II. THEORETICAL FORMALISM

In section IIA, we present the wave functions of the nucleon resonances $S_{11}(1535)$, $S_{11}(1650)$, $D_{13}(1520)$ and $D_{13}(1700)$. Section IIB embodies a brief review of the formalism for the strong decay of the baryon resonances to meson-baryon in a χ CQM, where we derive transition coupling amplitudes for the above four nucleon resonances to the πN , ηN , $K\Lambda$, $K\Sigma$ and $\eta' N$ channels.

A. Wave functions

In the χ CQM, complemented with five-quark components, a baryon is a superposition of three- and five-quark mixture and the wave function can be written as

$$|B\rangle = A_3|qqq\rangle + A_5|qqqq\bar{q}\rangle, \quad (1)$$

with A_3 and A_5 the probability amplitudes for the corresponding qqq and $qqqq\bar{q}$ states, respectively.

For the three-quark components, we employ the wave functions in traditional three-quark χ CQM. In the $SU(6) \otimes O(3)$ conserved case, the general form for the wave functions of the octet baryons, $N(8^2P_M)_{S^-}$ and $N(8^4P_M)_{S^-}$ states, can be expressed as

$$|B(8^2S_S)_{\frac{1}{2}^+}, S_z\rangle = \frac{1}{\sqrt{2}}(|B\rangle_\lambda|\frac{1}{2}, s_z\rangle_\lambda + |B\rangle_\rho|\frac{1}{2}, s_z\rangle_\rho)\varphi_{000}^s(\vec{\lambda}, \vec{\rho}), \quad (2)$$

$$|N(8^2P_M)_{S^-}, S_z\rangle = \frac{1}{2} \sum_{m, s_z} C_{1m, \frac{1}{2} s_z}^{SS_z} [(|N\rangle_\rho|\frac{1}{2}, s_z\rangle_\lambda + |N\rangle_\lambda|\frac{1}{2}, s_z\rangle_\rho)\varphi_{11m}^\rho(\vec{\lambda}, \vec{\rho}) \\ + (|N\rangle_\rho|\frac{1}{2}, s_z\rangle_\rho - |N\rangle_\lambda|\frac{1}{2}, s_z\rangle_\lambda)\varphi_{11m}^\lambda(\vec{\lambda}, \vec{\rho})], \quad (3)$$

$$|N(8^4P_M)_{S^-}, S_z\rangle = \frac{1}{\sqrt{2}} \sum_{m, s_z} C_{1m, \frac{3}{2} s_z}^{SS_z} [(|N\rangle_\rho|\frac{3}{2}, s_z\rangle_\rho)\varphi_{11m}^\rho(\vec{\lambda}, \vec{\rho}) + |N\rangle_\lambda|\frac{3}{2}, s_z\rangle_\lambda\varphi_{11m}^\lambda(\vec{\lambda}, \vec{\rho})], \quad (4)$$

where $|B\rangle_{\rho(\lambda)}$ denotes the mixed symmetric flavor wave function of the three-quark system for the corresponding baryon. $|\frac{1}{2}, s_z\rangle_{\rho(\lambda)}$ and $|\frac{3}{2}, s_z\rangle$ are the mixed symmetric and symmetric spin wave functions of the three-quark system, respectively. $\varphi_{Nlm}(\vec{\lambda}, \vec{\rho})$ is the harmonic oscillator basis orbital wave function for the three quarks with the subscripts Nlm being the corresponding quantum numbers. Finally, $C_{1m, ss_z}^{SS_z}$ are the Clebsch-Gordan coefficients for the coupling of the orbital and spin of the three-quark system to form a baryon state with spin S and z-component S_z . The explicit forms for all of the above flavor, spin, and orbital wave functions can be found in [54].

Taking into account the breakdown of $SU(6) \otimes O(3)$ symmetry due to either the color-magnetic [58] or flavor-magnetic [59] hyperfine interactions between the quarks, one can express the wave functions of the S_{11} and D_{13} resonances in terms of the given $N(8^2P_M)_{S^-}$ and $N(8^4P_M)_{S^-}$ wave functions, Eqs. (3) and (4), by introducing the configuration mixing angles θ_S and θ_D

$$\begin{pmatrix} |S_{11}(1535)\rangle \\ |S_{11}(1650)\rangle \end{pmatrix} = \begin{pmatrix} \cos\theta_S & -\sin\theta_S \\ \sin\theta_S & \cos\theta_S \end{pmatrix} \begin{pmatrix} |N(8^2P_M)_{\frac{1}{2}^-}\rangle \\ |N(8^4P_M)_{\frac{1}{2}^-}\rangle \end{pmatrix}, \quad (5)$$

$$\begin{pmatrix} |D_{13}(1520)\rangle \\ |D_{13}(1700)\rangle \end{pmatrix} = \begin{pmatrix} \cos\theta_D & -\sin\theta_D \\ \sin\theta_D & \cos\theta_D \end{pmatrix} \begin{pmatrix} |N(8^2P_M)_{\frac{3}{2}^-}\rangle \\ |N(8^4P_M)_{\frac{3}{2}^-}\rangle \end{pmatrix}. \quad (6)$$

For the octet baryons, other than the lowest lying S_{11} and D_{13} , the configuration mixing effects are not so significant. So, for those baryons we take the wave functions within the exact $SU(6) \otimes O(3)$ symmetry.

For the five-quark components of $S_{11}(1535)$, we use the wave functions given in Ref. [53],

$$\begin{aligned} \psi_{t,s} = & \sum_{a,b,c} \sum_{Y,y,T_z,t_z} \sum_{S_z,s_z} C_{[31]_a[211]_a}^{[14]} C_{[F]_b[S]_c}^{[31]_a} [F]_{b,Y,T_z} [S]_{c,S_z} [211; C]_a(Y, T, T_z, y, \bar{t}, t_z | 1, 1/2, t) \\ & (S, S_z, 1/2, s_z | 1/2, s) \bar{\chi}_{y,t_z} \bar{\xi}_{s_z} \varphi_{[5]}. \end{aligned} \quad (7)$$

In fact, this general wave function is appropriate for the five-quark components in all the low-lying nucleon resonances with $S^p = \frac{1}{2}^-$, albeit with different probabilities for five-quark components.

As reported in Ref. [53], there are 5 different flavor-spin configurations which may form five-quark components in the resonances with negative parity. If the hyperfine interaction between the quarks is assumed to depend on flavor and spin, the energy of the second and third configurations should be about 80 MeV and 200 MeV higher than the first configuration, respectively. Since $S_{11}(1535)$ and $S_{11}(1650)$ are the first two orbital excitations of the nucleon with spin 1/2, the configurations with low energies, namely the first two five-quark configurations should be the most appropriate ones to form higher Fock components in those two resonances. Moreover, the contribution of the second five-quark configuration is very similar to that of the first one, because of the same flavor structure, which rules out the five-quark components with light quark and anti-quark pairs in the S_{11} resonances. Actually, the transition elements between all of the 5 five-quark configurations and the octet baryons differ just by constant factors. Therefore, the contributions from all the 5 configurations are similar, albeit with appropriate probability amplitudes. Consequently, the first configuration is enough for us to study the strong decays of $S_{11}(1535)$ and $S_{11}(1650)$. Then the wave functions for the five-quark components in $S_{11}(1535)$ and $S_{11}(1650)$ reduce to the following form:

$$\psi_{5q} = \sum_{abc} C_{[31]_a[211]_a}^{[14]} C_{[211]_b[22]_c}^{[31]_a} [4]_X [211]_F(b) [22]_S(c) [211]_C(a) \bar{\chi}_{s_z} \varphi(\{\vec{\xi}_i\}), \quad (8)$$

the explicit form of which is given in Ref. [52].

Following Eq. (5), the introduction of five-quark wave functions leads to

$$|S_{11}(1535)\rangle = A_3 \left[\cos\theta_S |N(\frac{2}{8}P_M)_{\frac{1}{2}-}\rangle - \sin\theta_S |N(\frac{4}{8}P_M)_{\frac{1}{2}-}\rangle \right] + A_5 \psi_{5q}, \quad (9)$$

$$|S_{11}(1650)\rangle = A'_3 \left[\sin\theta_S |N(\frac{2}{8}P_M)_{\frac{1}{2}-}\rangle + \cos\theta_S |N(\frac{4}{8}P_M)_{\frac{1}{2}-}\rangle \right] + A'_5 \psi_{5q}. \quad (10)$$

The probability amplitude for the five-quark component in a baryon can be related to the

coupling ${}_{5q}\langle\hat{V}_{cou}\rangle_{3q}$ between the qqq and $qqqq\bar{q}$ configurations in the corresponding baryon

$$A_{5q} = \frac{{}_{5q}\langle\hat{V}_{cou}\rangle_{3q}}{M - E_5}, \quad (11)$$

with E_5 the energy of the five-quark component. Given that the resonances considered here have negative parity, all of the quarks and anti-quark in the five-quark system should be in their ground states. Hence, we can take \hat{V}_{cou} to be of the following form:

$$\hat{V}_{cou} = 3V(r_{34}) \frac{\vec{\sigma}_3 \cdot \vec{p}_3}{2m_3} \chi_{00}^{45} C_{00}^{45} F_{00}^{45} \varphi_{00}(\vec{p}_4 - \vec{p}_5) b_4^\dagger(\vec{p}_4) d_5^\dagger(\vec{p}_5), \quad (12)$$

where χ_{00}^{45} , C_{00}^{45} , F_{00}^{45} and $\varphi_{00}(\vec{p}_4 - \vec{p}_5)$ denote the spin, flavor, color and orbital singlets of the quark and anti-quark pair, respectively. $b_4^\dagger(\vec{p}_4)$ and $d_5^\dagger(\vec{p}_5)$ are the creation operators for a quark and anti-quark pair with momentum \vec{p}_4 and \vec{p}_5 , respectively. $V(r_{34})$ is the coupling potential which depends on the relative coordinate $|\vec{r}_3 - \vec{r}_4|$. Then we obtain

$$\frac{\langle\psi_{5q}|\hat{V}_{cou}|N(\frac{2}{8}P_M)_{\frac{1}{2}-}\rangle}{\langle\psi_{5q}|\hat{V}_{cou}|N(\frac{4}{8}P_M)_{\frac{1}{2}-}\rangle} = -2, \quad (13)$$

and

$$\frac{A'_{5q}}{A_{5q}} = \frac{\sin\theta_S - \frac{1}{2}\cos\theta_S}{\cos\theta_S + \frac{1}{2}\sin\theta_S} \frac{M_{S_{11}(1535)} - E_5}{M_{S_{11}(1650)} - E_5}. \quad (14)$$

Here we would like to emphasize that the considered D_{13} resonances are not relevant for five-quark components issues. Actually, all of the quarks and anti-quark should be in their ground states (lowest energy) to form the negative parity. Then the spin configuration of four-quark subsystem is limited to be $[31]_S$, for which the total spin of the four-quark subsystems is $S = 1$, in order to combine with the anti-quark to form the required total spin $3/2$. For the configurations with spin $[31]_S$, the flavor-spin overlap factors between such five-quark configurations and the D_{13} states vanish. Therefore, the probabilities for these five-quark components in the D_{13} resonances are 0. Some additional five-quark configurations, other than those given in Ref. [53], could also be considered, for instance, the configurations with the anti-quark orbitally excited ($l_{\bar{q}} = 2, 4 \dots$), the ones in which the four-quark subsystem with spin symmetry $[4]_S$ ($S_4 = 2$), or the ones given in Ref. [49] with the four quark subsystem orbital symmetry $[31]_X$ and orbital momentum $L_4 = 2, 4 \dots$. However, all those configurations have very high energies, far away from the lowest lying D_{13} resonances masses.

Finally, we do not consider the five-quark components in the ground states of octet baryons in this manuscript, because on the one hand their probabilities in the baryons are very small [48, 60], and on the other hand their contributions to electromagnetic and strong decays of nucleon resonances are negligible [52]. Actually, the five-quark configurations in the ground states of octet baryons cannot transit to three-quark components of the first orbitally excited baryon resonances due to the vanishing flavor-spin overlap factors.

B. Formalism for strong decay

It is well known that the pseudoscalar meson-quark coupling, in the tree level approximation, takes the form

$$H_M = \sum_j \frac{g_A^q}{2f_M} \bar{\psi}_j \gamma_\mu^j \gamma_5^j \psi_j \partial^\mu \phi_M, \quad (15)$$

where ψ_j and ϕ_M are the quark and pseudoscalar fields, respectively, and g_A^q is the axial coupling constant for the constituent quarks, the value of which is in the range $0.7 - 1.26$ [3, 61, 62]. f_M denotes the decay constant of the corresponding meson; the empirical values for the decay constants of π , K , η and η' are $f_\pi = 93$ MeV, $f_K = 113$ MeV, $f_\eta = 1.2f_\pi$, $f_{\eta'} = -0.58f_\pi$.

In the framework of non-relativistic qqq quark model, the coupling, Eq. (15), takes the following form:

$$H_M^{NR(3)} = \sum_j \frac{g_A^q}{2f_M} \left(\frac{\omega_M}{E_f + M_f} \sigma \cdot \vec{P}_f + \frac{\omega_M}{E_i + M_i} \sigma \cdot \vec{P}_i - \sigma \cdot \vec{k}_M + \frac{\omega_M}{2\mu} \sigma \cdot \vec{p}_j \right) X_M^j \exp\{-i\vec{k}_M \cdot \vec{r}_j\}. \quad (16)$$

Here, \vec{k}_M and ω_M are the three momentum and energy of the final meson, $\vec{P}_{i(f)}$ and $M_{i(f)}$ denote the mass and three momentum of the initial (final) baryon, \vec{p}_j and \vec{r}_j the three momentum and coordinate of the j^{th} quark, and μ is the reduced mass of the initial and final j^{th} quark which emits the meson. Finally, X_M^j is the flavor operator for emission of the meson from the corresponding j^{th} quark, given by following expressions:

$$\begin{aligned} X_{\pi^0}^j &= \lambda_3^j, \quad X_{\pi^\pm}^j = \mp \frac{1}{\sqrt{2}}(\lambda_1^j \mp \lambda_2^j), \\ X_{K^\pm}^j &= \mp \frac{1}{\sqrt{2}}(\lambda_4^j \mp \lambda_5^j), \quad X_{K^0}^j = \mp \frac{1}{\sqrt{2}}(\lambda_6^j \mp \lambda_7^j), \\ X_\eta^j &= \cos\theta \lambda_8^j - \sin\theta \sqrt{\frac{2}{3}} \mathcal{I}, \quad X_{\eta'}^j = \sin\theta \lambda_8^j + \cos\theta \sqrt{\frac{2}{3}} \mathcal{I}, \end{aligned} \quad (17)$$

where λ_i^j are the $SU(3)$ Gell-Mann matrices, and \mathcal{I} the unit operator in the $SU(3)$ flavor

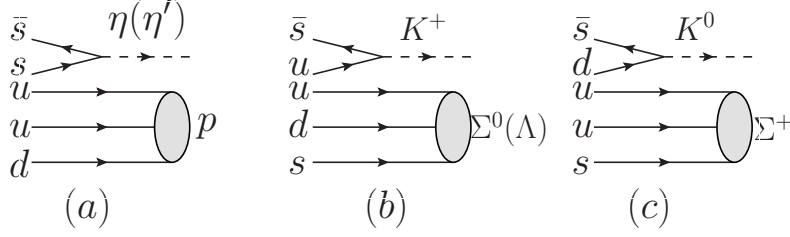


FIG. 1: (Color online) Strangeness component transit in the S_{11} resonances to ηp or $\eta' p$ (a), $K^+ \Lambda$ or $K^+ \Sigma^0$ (b) and $K^0 \Sigma^+$ (c).

space. θ denotes the mixing angle between η_1 and η_8 , leading to the physical η and η'

$$\eta = \eta_8 \cos \theta - \eta_1 \sin \theta, \quad (18)$$

$$\eta' = \eta_8 \sin \theta + \eta_1 \cos \theta, \quad (19)$$

it takes the value $\theta = -23^\circ$ [63].

Taking into account the five-quark components in the resonances, we have to calculate the transition coupling amplitudes for $qqqq\bar{q} \rightarrow qqq + M$. The reduced form of the coupling in Eq. (15) reads

$$H_M^{NR(5)} = \sum_j \frac{g_A^q}{2f_M} C_{XFS}^j(m_i + m_f) \bar{\chi}_z^\dagger \begin{pmatrix} 1 & 0 \\ 0 & 1 \end{pmatrix} \chi_z^j X_M^j \exp\{-i\vec{k}_M \cdot \vec{r}_j\}, \quad (20)$$

where m_i and m_f denote the constituent masses of the quark and anti-quark which combine to form a pseudoscalar meson, C_{XFS}^j denotes the overlap between the three-quark configuration of the final baryon and the residual orbital-flavor-spin-color configuration of the three-quark system that is left in the initial $qqqq\bar{q}$ after the combination of the j^{th} quark with the anti-quark into a final meson. The transitions $qqqs\bar{s} \rightarrow B + M$ scheme is shown in Fig. 1. where three quarks of the five-quark system go as spectators to form the final three-quark baryon, and the fourth quark gets combined with the strange anti-quark to form a meson: K , η or η' .

Then, the transition coupling amplitude for a resonance to a pseudoscalar meson and a octet baryon is obtained by calculating the following matrix element:

$$T^{MB} = \langle B(\frac{2}{3}S_S)_{\frac{1}{2}^+} | (H_M^{NR(3)} + H_M^{(5)}) | N^* \rangle \equiv T_3^{MB} + T_5^{MB}, \quad (21)$$

the resulting transition coupling amplitudes T_3^{MB} and T_5^{MB} for the S_{11} and D_{13} resonances to $\pi^0 p$, $\pi^+ n$, ηp , $K^+ \Lambda$, $K^0 \Sigma^+$, $K^+ \Sigma^0$ and $\eta' p$ channels are shown in Tables I and II, respectively.

TABLE I: Transition coupling amplitudes T_3^{MB} for the low-lying S_{11} and D_{13} resonances to meson-baryon final states. Note that the full amplitudes are obtained by multiplying each term by the following expressions: $\frac{g_A^q}{2f_M}\omega_3[(a_M - \frac{b_M}{3})\frac{k_M^2}{\omega_3^2} - 3b_M]\exp\{-\frac{k_M^2}{6\omega_3^2}\}$ for S_{11} and $\frac{g_A^q}{2f_M}(a_M - \frac{b_M}{3})\frac{k_M^2}{\omega_3}\exp\{-\frac{k_M^2}{6\omega_3^2}\}$ for D_{13} resonances. Here, ω_3 is the harmonic oscillator parameter for the three-quark components, $a_M = 1 + \frac{\omega_M}{E_f + M_f}$ and $b_M = \frac{\omega_M}{2\mu}$.

	$S_{11}(1535)$	$S_{11}(1650)$
$\pi^0 p$	$\frac{\sqrt{2}}{9}(2\cos\theta_S - \sin\theta_S)$	$\frac{\sqrt{2}}{9}(2\sin\theta_S + \cos\theta_S)$
$\pi^+ n$	$-\frac{2}{9}(2\cos\theta_S - \sin\theta_S)$	$-\frac{2}{9}(2\sin\theta_S + \cos\theta_S)$
ηp	$\frac{\sqrt{2}}{3}(\cos\theta_S + \sin\theta_S)(\frac{1}{\sqrt{3}}\cos\theta - \sqrt{\frac{2}{3}}\sin\theta)$	$\frac{\sqrt{2}}{3}(\sin\theta_S - \cos\theta_S)(\frac{1}{\sqrt{3}}\cos\theta - \sqrt{\frac{2}{3}}\sin\theta)$
$K^0 \Lambda$	$-\frac{1}{\sqrt{6}}\cos\theta_S$	$-\frac{1}{\sqrt{6}}\sin\theta_S$
$K^0 \Sigma^+$	$-\frac{1}{9}(\cos\theta_S + 4\sin\theta_S)$	$-\frac{1}{9}(\sin\theta_S - 4\cos\theta_S)$
$K^+ \Sigma^0$	$-\frac{1}{9\sqrt{2}}(\cos\theta_S + 4\sin\theta_S)$	$-\frac{1}{9\sqrt{2}}(\sin\theta_S - 4\cos\theta_S)$
$\eta' p$	$\frac{\sqrt{2}}{3}(\cos\theta_S + \sin\theta_S)(\frac{1}{\sqrt{3}}\sin\theta + \sqrt{\frac{2}{3}}\cos\theta)$	$\frac{\sqrt{2}}{3}(\sin\theta_S - \cos\theta_S)(\frac{1}{\sqrt{3}}\sin\theta + \sqrt{\frac{2}{3}}\cos\theta)$
	$D_{13}(1520)$	$D_{13}(1700)$
$\pi^0 p$	$-\frac{2}{9}(2\cos\theta_D - \frac{1}{\sqrt{10}}\sin\theta_D)$	$-\frac{2}{9}(2\sin\theta_D + \frac{1}{\sqrt{10}}\cos\theta_D)$
$\pi^+ n$	$\frac{2\sqrt{2}}{9}(2\cos\theta_D - \frac{1}{\sqrt{10}}\sin\theta_D)$	$\frac{2\sqrt{2}}{9}(2\sin\theta_D + \frac{1}{\sqrt{10}}\cos\theta_D)$
ηp	$-\frac{2}{3}(\cos\theta_D + \frac{1}{\sqrt{10}}\sin\theta_D)(\frac{1}{\sqrt{3}}\cos\theta - \sqrt{\frac{2}{3}}\sin\theta)$	$-\frac{2}{3}(\sin\theta_D - \frac{1}{\sqrt{10}}\cos\theta_D)(\frac{1}{\sqrt{3}}\cos\theta - \sqrt{\frac{2}{3}}\sin\theta)$
$K^0 \Lambda$	$\frac{1}{\sqrt{3}}\cos\theta_D$	$\frac{1}{\sqrt{3}}\sin\theta_D$
$K^0 \Sigma^+$	$\frac{1}{9}(\sqrt{2}\cos\theta_D + \frac{4}{\sqrt{5}}\sin\theta_D)$	$\frac{1}{9}(\sqrt{2}\sin\theta_D - \frac{4}{\sqrt{5}}\cos\theta_D)$
$K^+ \Sigma^0$	$-\frac{1}{9\sqrt{2}}(\sqrt{2}\cos\theta_D + \frac{4}{\sqrt{5}}\sin\theta_D)$	$-\frac{1}{9\sqrt{2}}(\sqrt{2}\sin\theta_D - \frac{4}{\sqrt{5}}\cos\theta_D)$
$\eta' p$	$-\frac{2}{3}(\cos\theta_D + \frac{1}{\sqrt{10}}\sin\theta_D)(\frac{1}{\sqrt{3}}\sin\theta + \sqrt{\frac{2}{3}}\cos\theta)$	$-\frac{2}{3}(\sin\theta_D - \frac{1}{\sqrt{10}}\cos\theta_D)(\frac{1}{\sqrt{3}}\sin\theta + \sqrt{\frac{2}{3}}\cos\theta)$

Notice that (Table I), within the exact $SU(6) \otimes O(3)$ symmetry, the matrix elements for transition $N(\frac{4}{8}P_M)_{S^-} \rightarrow K\Lambda$ vanish, and hence the decay widths of $S_{11}(1650)$ and $D_{13}(1700)$ to $K\Lambda$ are null. Moreover, Table II, the transition elements for $5q \rightarrow MB$ do not vanish when $k_M = 0$, and it may enhance or depress the transitions $S_{11} \rightarrow MB$ significantly near the meson-baryon threshold. Finally, the strangeness component does not transit to $\pi^0 p$, since the matrix element of the flavor operator $X_{\pi^0}^j$ between the $s\bar{s}$ pair is 0.

To obtain the relevant expressions for partial decay widths, we take the Lagrangian for N^*MB coupling in hadronic level to be of the following form:

$$\mathcal{L}_{S_{11}BM} = -ig_{S_{11}BM}\bar{\psi}_B\phi_M\psi_{S_{11}} + h.c., \quad (22)$$

TABLE II: Transition coupling amplitudes T_5^{MB} . Note that the full amplitudes are obtained by multiplying each term by the following expression: $\frac{g_A}{2f_M}C_{35}\exp\{-\frac{3k_M^2}{20\omega_5^2}\}$, with C_{35} related to the harmonic oscillator parameter for the three- and five-quark components as $C_{35} = (\frac{2\omega_3\omega_5}{\omega_3^2+\omega_5^2})^3$.

$\pi^0 p$	$\pi^+ n$	ηp	$K^+ \Lambda$	$K^0 \Sigma^+$	$K^+ \Sigma^0$	$\eta' p$
0	0	$\frac{2}{\sqrt{3}}m_s(2\cos\theta + \sqrt{2}\sin\theta)$	$\frac{1}{\sqrt{3}}(m + m_s)$	$\sqrt{2}(m + m_s)$	$-(m + m_s)$	$\frac{2}{\sqrt{3}}m_s(2\sin\theta - \sqrt{2}\cos\theta)$

$$\mathcal{L}_{D_{13}BM} = \frac{1}{m_M} g_{D_{13}BM} \bar{\psi}_B \partial_\mu \phi_M \psi_{D_{13}}^\mu + h.c., \quad (23)$$

where $\bar{\psi}_B$ and $\psi_{S_{11}}$ denote the Dirac spinor fields for the final baryon and the S_{11} resonances, respectively, and ϕ_M is the scalar field for the final meson.

For the D_{13} resonances, with spin 3/2, we employ the Rarita-Schwinger vector-spinor fields $\psi_{D_{13}}^\mu$ [64, 65], which are defined as

$$\psi_{D_{13}}^\mu(S_z) = \sum_{ms} C_{1m, \frac{1}{2}s}^{\frac{3}{2}S_z} \epsilon_m^\mu u_s. \quad (24)$$

One can directly obtain the transition coupling amplitudes for $N^* \rightarrow MB$ in the hadronic level using the Lagrangian, Eq. (23). Then, the coupling constants g_{N^*MB} are extracted by comparing the transition coupling amplitudes T^{MB} in the quark model to those in the hadronic model.

With the resulting coupling constants, the strong decay widths for the S_{11} and D_{13} resonances to the pseudoscalar meson and octet baryon read

$$\Gamma_{S_{11} \rightarrow MB} = \frac{1}{4\pi} g_{S_{11}MB}^2 \frac{E_f + M_f}{M_i} |\vec{k}_M|, \quad (25)$$

$$\Gamma_{D_{13} \rightarrow MB} = \frac{1}{12\pi} \frac{1}{m_M^2} g_{D_{13}MB}^2 \frac{E_f - M_f}{M_i} |\vec{k}_M|^3. \quad (26)$$

Note that in the center of mass frame of the initial resonance, $\vec{P}_i = 0$, \vec{k}_M and E_f can be related to the masses of the initial and final hadrons as

$$|\vec{k}_M| = |\vec{P}_f| = \frac{\sqrt{[M_i^2 - (M_f + m_M)^2][M_i^2 - (M_f - m_M)^2]}}{2M_i}, \quad (27)$$

$$E_f = \sqrt{|\vec{k}_M|^2 + M_f^2} = \frac{M_i^2 - m_M^2 + M_f^2}{2M_i}. \quad (28)$$

For decay channels with thresholds above the mass of the initial resonance, off-shell effects are taken into account by putting $|\vec{k}_M| = 0$ and introducing the form factor [4]

$$F = \frac{\Lambda^4}{\Lambda^4 + (q_{N^*}^2 - M_{N^*}^2)^2}, \quad (29)$$

with the cutoff parameter $\Lambda = 1$ GeV, and q_{N^*} the threshold of the corresponding channel. In fact, this form factor affects mainly the $N^* \rightarrow \eta' N$ process, since thresholds for all other channels are below or slightly above the masses of the four resonances.

III. NUMERICAL RESULTS

In this section our results for partial decay widths $\Gamma_{N^* \rightarrow MB}$ and coupling constants $g_{N^* MB}$ are reported for the four investigated resonances, with $MB \equiv \pi^0 p, \pi^+ n, \eta p, K^+ \Lambda, K^0 \Sigma^+, K^+ \Sigma^0$ and $\eta' p$.

The starting point, section III A, is the standard χ CQM. Then, in section III B we introduce $SU(6) \otimes O(3)$ breaking and finally, in section III C, the five-quark components are embodied for the S_{11} resonances.

For the partial decay widths, we compare our results to the experimental values reported in PDG [1], and produce predictions for yet unmeasured channels.

A. Pure qqq configuration and exact $SU(6) \otimes O(3)$ symmetry

Within this simplest configuration, there are three input parameters: quarks' masses and harmonic oscillator parameter.

For the constituent quarks' masses, we use the traditional qqq quark model values [31, 35, 59], namely, $m \equiv m_u = m_d = 340$ MeV and $m_s = 460$ MeV.

The scale of the oscillator parameter, ω_3 , can be inferred from the empirical radius of the proton via $\omega_3 = 1/\sqrt{\langle r^2 \rangle}$, which leads to $\omega_3 \simeq 250$ MeV, for $\sqrt{\langle r^2 \rangle} \simeq 1$ fm. However, since the photon couples to u and d quarks through ρ and ω mesons, the measured proton charge radius may reflect partly the vector meson propagator [66]. Moreover, pion cloud have some influence on the measured proton charge radius. Consequently, the intrinsic size of the proton still has some model dependence, and hence, the oscillator parameter ω_3 might deviate from 250 MeV, within the range 100 – 400 MeV [31, 35, 48, 50].

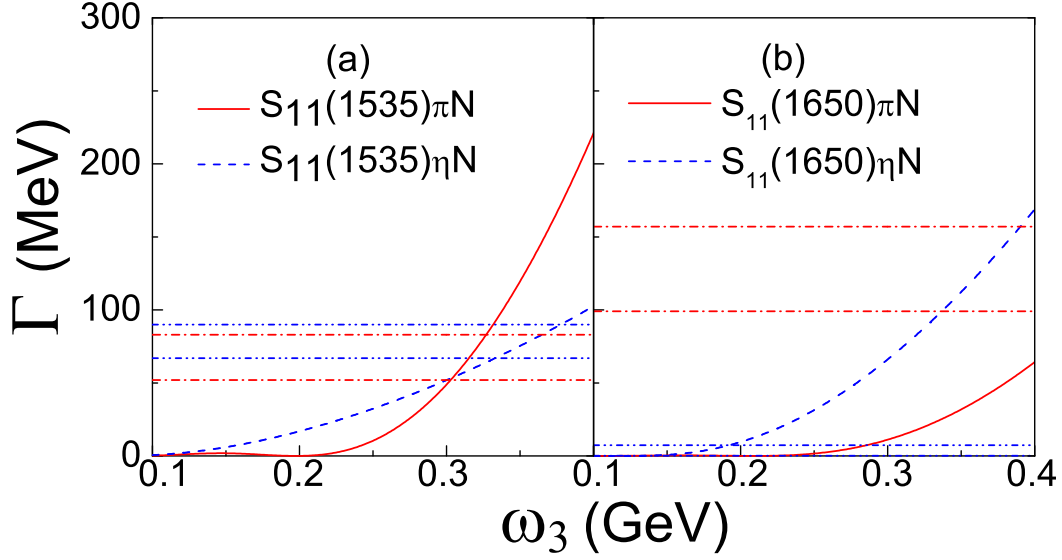


FIG. 2: (Color online) Partial decay widths of $S_{11}(1535)$ and $S_{11}(1650)$ to πN and ηN channels as a function of the harmonic oscillator parameter ω_3 . Results of the present work are depicted in full and dashed curves for $S_{11} \rightarrow \pi N$ and $S_{11} \rightarrow \eta N$, respectively, without the $SU(6) \otimes O(3)$ breakdown effects. The horizontal lines are the bands given in PDG, for $S_{11} \rightarrow \pi N$ (dash-dotted) and $S_{11} \rightarrow \eta N$ (dash-dot-dotted).

Figure 2 shows the decay widths for $S_{11}(1535) \rightarrow \pi N$, ηN (left panel) and $S_{11}(1650) \rightarrow \pi N$, ηN (right panel) as a function of ω_3 . The full and dashed curves are our results and the horizontal lines give the bands reported in PDG [1].

The width for $S_{11}(1535) \rightarrow \pi N$ (full curve) falls in the experimental range (dash-dotted lines) for $300 \lesssim \omega_3 \lesssim 340$ MeV, while for $S_{11}(1535) \rightarrow \eta N$ the dashed curve and dash-dot-dotted lines lead to $300 \lesssim \omega_3 \lesssim 380$ MeV. Accordingly, in the former range for ω_3 , the simple qqq configuration allows reproducing the decay widths of $S_{11}(1535)$ in both πN and ηN channels.

The situation with respect to the second S_{11} resonance is dramatically different. In the whole ω_3 range, the calculated $S_{11}(1650) \rightarrow \pi N$ width (full curve), underestimates the experimental band (dash-dotted lines). For the ηN decay channel, predicted values (dashed curve) agree with experimental band (dash-dot-dotted lines) below $\omega_3 \approx 200$ MeV, where $\Gamma_{S_{11}(1650) \rightarrow \pi N}$ turns out vanishing.

It is also worthwhile mentioning that, within exact $SU(6) \otimes O(3)$ symmetry,

$\Gamma_{S_{11}(1650) \rightarrow K\Lambda} = 0$ and hence, disagrees with the experimental value [1]: 4.8 ± 0.7 MeV.

In summary the pure qqq configuration, within exact $SU(6) \otimes O(3)$, is not appropriate in describing the $S_{11}(1650)$ resonance properties. Consequently, one has to consider the $SU(6) \otimes O(3)$ breakdown effects.

B. Pure qqq configuration and broken $SU(6) \otimes O(3)$ symmetry

As discussed in section II A, $SU(6) \otimes O(3)$ symmetry breaking effects can be related to the mixing angles θ_S and θ_D . Several predictions on those angles are available (for a recent review see e.g. Ref. [67]). Here, we will extract ranges for both angles and discuss them with respect to the two most common approaches leading to $SU(6) \otimes O(3)$ symmetry breaking, namely, one-gluon-exchange (OGE) [31, 68–72] and one-boson-exchange models (OBE) [59]. Those approaches have raised some controversy [73, 74]. Given that both the sign and the magnitude of the mixing angles in those approaches are different (see e.g. Refs. [67, 75]), and that even within a given approach, the sign depends on the convention used [31, 67] or on the exchanged mesons included [76], we give in Appendix A values obtained within each approach in line with the de Swart [77] convention for $SU(3)$.

In order to investigate the sign and range for θ_S , in this section we report our numerical results for partial decay widths of $S_{11}(1535)$ and $S_{11}(1650)$ to πN and ηN as a function of ω_3 for six values of θ_S , namely, $\pm 15^\circ$, $\pm 30^\circ$, $\pm 45^\circ$, and compare them to the data ranges.

In Fig. 3 the strong decay partial widths $\Gamma_{S_{11} \rightarrow \pi N}$ and $\Gamma_{S_{11} \rightarrow \eta N}$ for $S_{11}(1535)$ (upper panel) and $S_{11}(1650)$ (lower panel) are shown as a function of ω_3 , with negative values for θ_S . Conventions for the curves are the same as in Fig. 2, and due to $SU(6) \otimes O(3)$ symmetry breaking, $\Gamma_{S_{11}(1650) \rightarrow K\Lambda}$ gets non-vanishing values, depicted in dotted curves. The experimental bands for this latter width are not shown, because they are almost identical to those for $\Gamma_{S_{11}(1650) \rightarrow \eta N}$.

At all the three mixing angles, our predictions for $\Gamma_{S_{11}(1535) \rightarrow \pi N}$ and $\Gamma_{S_{11}(1650) \rightarrow \eta N}$ fall in the experimental bands for $\omega_3 \approx 300$ MeV, while the model underestimates very badly $\Gamma_{S_{11}(1535) \rightarrow \eta N}$ and $\Gamma_{S_{11}(1650) \rightarrow \pi N}$. Accordingly, within our approach, negative values for θ_S lead to unacceptable results compared to the data.

In Fig. 4 the strong decay partial widths $\Gamma_{S_{11} \rightarrow \pi N}$ and $\Gamma_{S_{11} \rightarrow \eta N}$ for both S_{11} resonances, as well as $\Gamma_{S_{11}(1650) \rightarrow K\Lambda}$, are depicted as a function of ω_3 with positive values for θ_S . For the

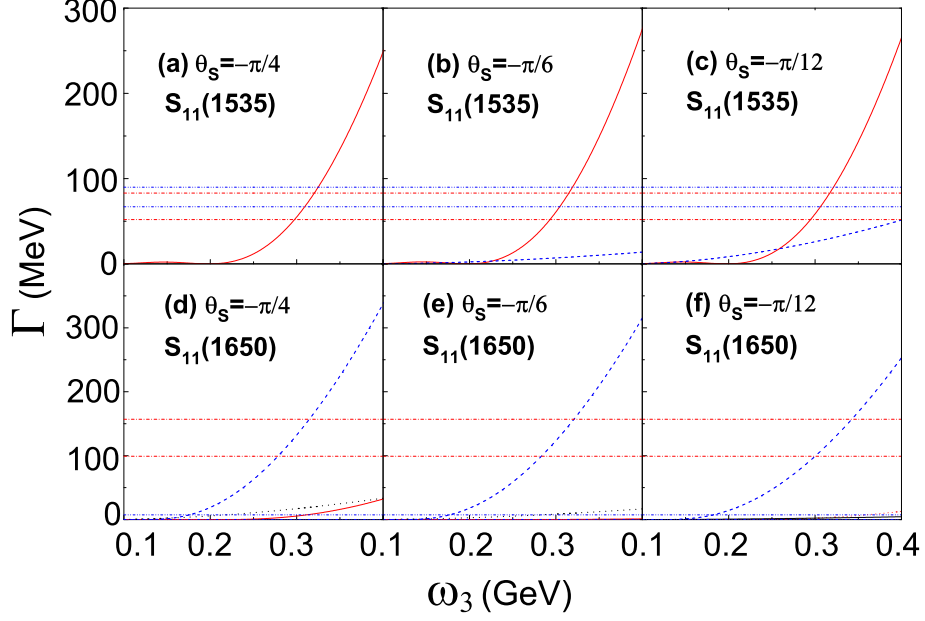


FIG. 3: (Color online) Decay widths of $S_{11}(1535)$ (upper panel) and $S_{11}(1650)$ (lower panel) as a function of ω_3 , with θ_S taken to be $-\frac{\pi}{4}$, $-\frac{\pi}{6}$ and $-\frac{\pi}{12}$, respectively. The dotted curves are our results for $\Gamma_{S_{11}(1650) \rightarrow K\Lambda}$, and the other ones are as in Fig. 2.

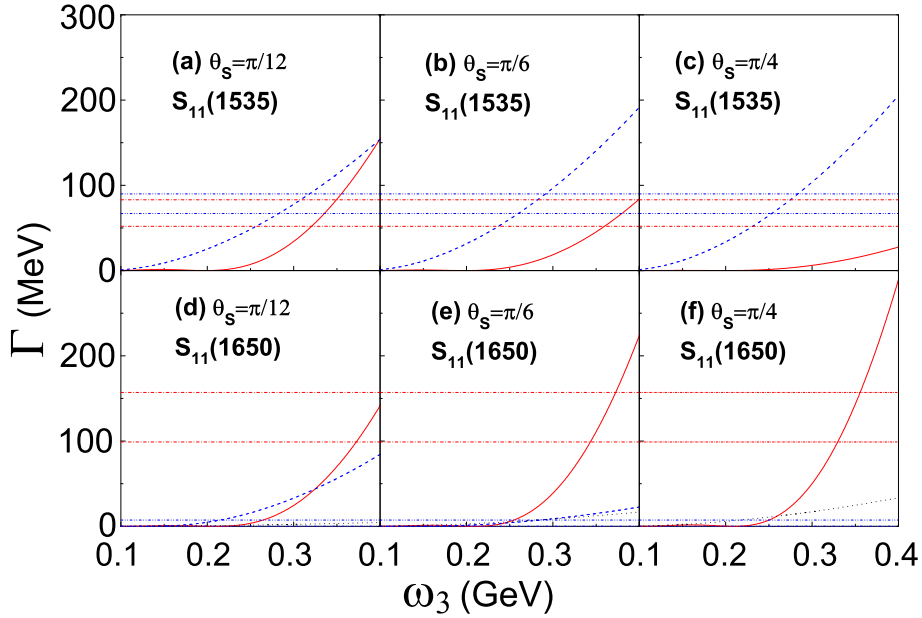


FIG. 4: (Color online) Same as Fig. 3, but with θ_S taken to be $\frac{\pi}{12}$, $\frac{\pi}{6}$ and $\frac{\pi}{4}$.

$S_{11}(1535)$ resonance, we obtain good agreement with data for $\theta_S = 15^\circ$ and $\omega_3 \approx 300$ MeV, for both πN and ηN decay widths. This is also the case at all angles for $S_{11}(1650) \rightarrow \pi N$, but for $\omega_3 \approx 350$ MeV.

To go further in our investigation, we fix the harmonic parameter at $\omega_3 = 340$ MeV and calculate partial widths and coupling constants for two extreme positive values of the mixing angle, $\theta_S = 15^\circ$ and 35° . Moreover, we extend our study to the $D_{13}(1520)$ and $D_{13}(1700)$ resonances, with the relevant mixing angle, also at two extreme values, $\theta_D = 0^\circ$ and 17.5° . Results obtained within this procedure are hereafter referred to as model A.

TABLE III: Strong decay partial widths (in MeV) for the S_{11} and D_{13} resonances in the three-quark model, with broken $SU(6) \otimes O(3)$ symmetry.

N^*	Γ_{tot}	πN	ηN	$K\Lambda$	Ref.
$S_{11}(1535)$	150 ± 25	68 ± 15	79 ± 11		PDG [1]
		51 ± 21	121 ± 15		Model A
$S_{11}(1650)$	165 ± 20	128 ± 29	3.8 ± 3.6	4.8 ± 0.7	PDG [1]
		81 ± 22	28 ± 22	9 ± 6	Model A
$D_{13}(1520)$	115 ± 15	69 ± 6	0.26 ± 0.05		PDG [1]
		66 ± 7	0.19 ± 0.01		Model A
		72 ± 11	0.26 ± 0.07		Jayalath <i>et al.</i> [46]
$D_{13}(1700)$	100 ± 50	10 ± 5	0.5 ± 0.5	1.5 ± 1.5	PDG [1]
		13 ± 10	0.5 ± 0.5	0.1 ± 0.1	Model A
		12 ± 13	≤ 0.15	≤ 0.03	Jayalath <i>et al.</i> [46]

In Table III, we present our results for the strong decay partial widths $\Gamma_{\pi N}$, $\Gamma_{\eta N}$ and $\Gamma_{K\Lambda}$ for the low lying S_{11} and D_{13} resonances studied here.

Within model A, the reduced χ^2 per data point is 10.3. However, this large value is due to $S_{11} \rightarrow \eta N$, $K\Lambda$ decay channels. It is worthwhile mentioning that for the five D_{13} partial decay widths, we get $\chi^2_{d.p.} = 0.7$.

Here, $\Gamma_{S_{11}(1535) \rightarrow \pi N}$ is well reproduced, while $\Gamma_{S_{11}(1535) \rightarrow \eta N}$ is overestimated at the level of

3σ and $\Gamma_{S_{11}(1650) \rightarrow \pi N}$ underestimated by roughly 2σ . For the remaining two other channels, large uncertainties on $\Gamma_{S_{11}(1650) \rightarrow \eta N}$ (both experiment and model), and on $\Gamma_{S_{11}(1650) \rightarrow K \Lambda}$ (mainly model) do not lead to reliable conclusions. Because of those undesirable features, we postpone to the next section the discussion on results from other sources, as well as the extraction of coupling constants.

For both D_{13} resonances, the model A allows reproducing satisfactorily enough (Table III) the known partial widths, and agrees with values obtained within the $1/N_C$ expansion framework [46]. model A is hence appropriate to put forward predictions for D_{13} -meson-baryon coupling constants. In Table IV, our predictions for $\Gamma_{D_{13}MB}$ for seven meson-baryon sets are reported.

TABLE IV: Coupling constants for D_{13} resonances to pseudoscalar meson and octet baryon within model A.

N^*	$\pi^0 p$	$\pi^+ n$	ηp	$K^+ \Lambda$	$K^0 \Sigma^+$	$K^+ \Sigma^0$	$\eta' p$
$D_{13}(1520)$	-1.51 ± 0.07	2.13 ± 0.10	-8.33 ± 0.20	3.44 ± 0.08	0.99 ± 0.14	-0.69 ± 0.09	2.11 ± 0.05
$D_{13}(1700)$	-0.35 ± 0.17	0.50 ± 0.25	0.93 ± 0.91	1.43 ± 1.43	-2.80 ± 0.05	1.98 ± 0.04	1.67 ± 0.52

To end this section, we summarize our main findings within a traditional qqq χ CQM, complemented with $SU(6) \otimes O(3)$ breakdown effects, and using following input values for adjustable parameters: $\omega_3 = 340$ MeV, $15^\circ \leq \theta_S \leq 35^\circ$ and $0^\circ \leq \theta_D \leq 17.5^\circ$.

Model A is found appropriate for the D_{13} resonances, given that the partial decay widths show from reasonable to good agreements with the PDG values. So, we do not push further our studies with respect to the $D_{13}(1520)$ and $D_{13}(1700)$.

The main shortcomings of the model A concern: $\Gamma_{S_{11}(1535) \rightarrow \eta N}$ and the fact that for the $S_{11}(1650)$ resonance, central values for all three channels show significant discrepancies with those reported in PDG. This latter point remains problematic because of large uncertainties.

Attempting to cure those disagreements with respect to the S_{11} resonances, we proceed in the next section to considering possible contributions from higher Fock-components.

C. Mixed qqq and $qqqq\bar{q}$ configuration and broken $SU(6) \otimes O(3)$ symmetry

To produce numerical results, seven input parameters are needed, the values of which are discussed below.

a) *Constituent quarks' masses*: due to the introduction of five-quark components, masses to be used are smaller than those we adopted in section III A, while dealing with pure three-quark states. In line with Ref. [52], we take $m = 290$ MeV and $m_s = 430$ MeV.

b) *Oscillator parameters*: following results presented in section III A, we fix the oscillator parameter at $\omega_3 = 340$ MeV. For the five-quark components a commonly used value for the oscillator parameter, $\omega_5 = 600$ MeV, is adopted.

c) *Mixing angle*: in Section III B, we showed that to fit the decay widths, the mixing angle should be in the range $15^\circ \leq \theta_S \leq 35^\circ$. In the following, this angle is treated as adjustable parameter.

d) *Probabilities of five-quark components*: the probabilities of the five-quark components in $S_{11}(1535)$ ($P_{5q} = A_{5q}^2$) and $S_{11}(1650)$ ($P'_{5q} = A_{5q}'^2$) are also adjustable parameters in our model search.

The latter three adjustable parameters have been extracted by mapping out the whole phase space defined by $15^\circ \leq \theta_S \leq 35^\circ$ and from 0 to 100% for five-quark probabilities in both $S_{11}(1535)$ and $S_{11}(1650)$. The calculated observables are: the partial decay widths of both S_{11} resonances to πN and ηN , as well as $\Gamma_{S_{11}(1650) \rightarrow K\Lambda}$. Sets $[\theta_S, P_{5q}, P'_{5q}]$ leading [78] to decay widths within ranges reported in PDG have been singled out. Then, for each partial widths, extreme values for those parameters are retained as model ranges, namely,

$$26.8^\circ \leq \theta_S \leq 29.8^\circ ; 21\% \leq P_{5q} \leq 30\% ; 11\% \leq P'_{5q} \leq 18\% . \quad (30)$$

The obtained model is hereafter called model B.

As an example, Fig. 5 illustrates how the known ranges for the partial decay widths allow determining ranges for the five-quark components' probabilities. There, for each decay width intersections of the model curve with the horizontal bands taken from PDG, determine the extreme values for the relevant five-quark probability.

Notice that the probability range for five-quark component in $S_{11}(1535)$ given above is compatible with previous results [52, 53], obtained within χCQM approaches. The latter one [53] puts an upper limit of $P_{5q} \leq 45\%$, based on the axial charge study of the resonance. While the former one [52], dedicated to the electromagnetic transition $\gamma^* N \rightarrow S_{11}(1535)$, reports $25\% \leq P_{5q} \leq 65\%$.

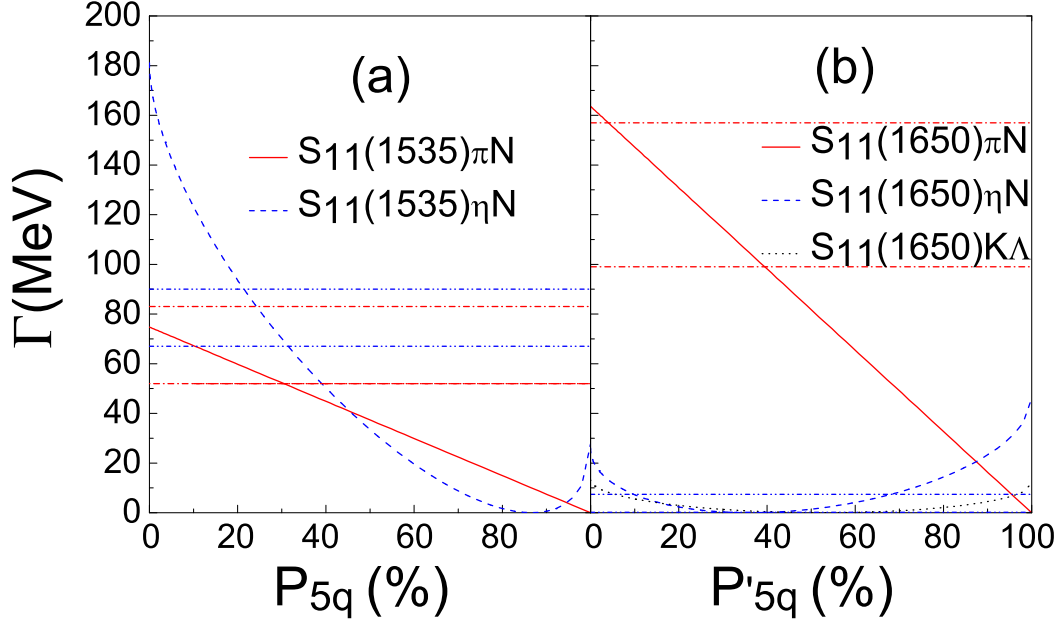


FIG. 5: (Color online) Partial decay widths (in MeV) for S_{11} resonances as a function of five-quark components, $\theta_S = 28^\circ$. Curves the same as in Fig. 4.

1. Partial decay widths $\Gamma_{S_{11} \rightarrow MB}$

The resulting numerical partial decay widths, within both models A and B, are reported in Table V and compared with the PDG data [1] as well as with results from other authors, based on various approaches [4, 6, 7, 14, 20, 22, 26, 38, 46].

Comparing results of the models A and B with the data for all five channels, shows clearly the superiority of the model B. The $\chi^2_{d.p.}$ is 0.15, instead of 19.9 in the case of model A.

The most striking feature here is that $\Gamma_{S_{11}(1535) \rightarrow \eta N}$ is nicely reproduced, which was not the case with previous configurations, namely, pure qqq without or with $SU(6) \otimes O(3)$ symmetry breaking. Moreover, $\Gamma_{S_{11}(1535) \rightarrow \pi N}$ agrees with PDG values within better than 1σ . The range for $\Gamma_{S_{11}(1650) \rightarrow \pi N}$ gets significantly reduced within the model B with respect to the model A result and is compatible with the PDG value within less than 1σ . Narrow experimental widths for $\Gamma_{S_{11}(1650) \rightarrow \eta N}$ and $\Gamma_{S_{11}(1650) \rightarrow K\Lambda}$ are well reproduced by the model B, with uncertainties comparable to those of the data. In the following, we proceed to comparisons with results from other sources.

The most complete set of results comes from a very recent comprehensive study [46] of all known partial decay widths for sixteen baryon resonances, within the framework of the

TABLE V: Strong decay widths (in MeV) for $S_{11}(1535)$ and $S_{11}(1650)$.

N^*	Γ_{tot}	πN	ηN	$K\Lambda$	Approach	Ref.
$S_{11}(1535)$	150 ± 25	68 ± 15	79 ± 11			PDG [1]
		51 ± 21	121 ± 15		Model A	Present work
		58 ± 5	79 ± 11		Model B	Present work
		57 ± 19	73 ± 44		$1/N_C$ -NLO	Jayalath <i>et al.</i> [46]
	112 ± 19	39 ± 5	57 ± 6		Coupled-channel	Vrana <i>et al.</i> [14]
	129 ± 8	46 ± 1	68 ± 1		Coupled-channel	Penner-Mosel [4]
	136	34.4	56.2		Coupled-channel	Shyam [20]
		42 ± 6	70 ± 10		PWA	Arndt <i>et al.</i> [22]
		21.3	65.7		Chiral Unitary	Inoue <i>et al.</i> [6]
	95	42	51		Chiral quark model	Golli <i>et al.</i> [38]
	165	64	89		K-Matrix	Ceci <i>et al.</i> [26]
	142		71		Disp. Rel.	Aznauryan [7]
	195		97		Isobar	Aznauryan [7]
$S_{11}(1650)$	165 ± 20	128 ± 29	3.8 ± 3.6	4.8 ± 0.7		PDG [1]
		81 ± 22	28 ± 22	9 ± 6	Model A	Present work
		143 ± 5	4.5 ± 3.0	4.8 ± 0.7	Model B	Present work
	202 ± 40	149 ± 4	12 ± 2		Coupled-channel	Vrana <i>et al.</i> [14]
	138 ± 7	90 ± 6	1.4 ± 0.8	3.7 ± 0.6	Coupled-channel	Penner-Mosel [4]
	133	71.9	2.5		Coupled-channel	Shyam [20]
	144	86	1.4	13	Chiral quark model	Golli <i>et al.</i> [38]
	233	149	37		K-Matrix	Ceci <i>et al.</i> [26]
	85		3.2		Disp. Rel.	Aznauryan [7]
	125		6.9		Isobar	Aznauryan [7]

$1/N_C$ expansion in the next to leading order (NLO) approximation. Results for the $S_{11}(1535)$ decay channels from that work and model B are in excellent agreement. For the $S_{11}(1650)$, given that the authors of Ref. [46] use branching fractions data in PDG for ηN and $K\Lambda$ channels, rather than the branching ratios, we postpone the comparisons to sec. III C 3.

The Pitt-ANL [14] multichannel analysis of $\pi N \rightarrow \pi N$, ηN , produces rather small total widths for $S_{11}(1535)$ and large one for $S_{11}(1650)$. Those features lead to underestimate of $\Gamma_{S_{11}(1535) \rightarrow \pi N}$ and $\Gamma_{S_{11}(1535) \rightarrow \eta N}$, and overestimate of $\Gamma_{S_{11}(1650) \rightarrow \eta N}$. However, $\Gamma_{S_{11}(650) \rightarrow \pi N}$ comes out in agreement with PDG and model B results.

An extensive coupled-channels analysis [4, 5] studied within an isobar approach all available data by year 2002 for following processes: $\gamma N \rightarrow \gamma N$, πN , $\pi\pi N$, ηN , $K\Lambda$, $K\Sigma$, ωN and $\pi N \rightarrow \pi N$, ηN , $K\Lambda$, $K\Sigma$, ωN . That work describes successfully four out of the five decay channels, albeit with a few tens of free parameters, with the main shortcoming being

the underestimate of $\Gamma_{S_{11}(1535) \rightarrow \pi N}$.

Interpreting $pN \rightarrow pN\eta$ data, within an effective Lagrangian approach [20], underestimates all partial decay widths, except $\Gamma_{S_{11}(1650) \rightarrow K\Lambda}$.

The latest available results from SAID [22], in 2005, analyzing πN elastic scattering and ηN production data, give a smaller $\Gamma_{S_{11}(1535) \rightarrow \pi N}$ with respect to PDG, and compatible with PDG value for $\Gamma_{S_{11}(1535) \rightarrow \eta N}$.

A chiral unitary approach [6] dedicated to the S -wave meson-baryon interactions, reproduces well $\Gamma_{S_{11}(1535) \rightarrow \eta N}$, but underestimates $\Gamma_{S_{11}(1535) \rightarrow \pi N}$ by more than a factor of 2.

A recent chiral quark model [38], concentrating on the meson scattering and π and η electroproduction amplitudes, leads to rather small total width for both resonances, underestimating all πN and ηN partial decay widths by roughly 2σ , and overestimating $\Gamma_{S_{11}(1650) \rightarrow K\Lambda}$ by more than 10σ . The authors conclude however that the $S_{11}(1535)$ resonance is dominated by a genuine three-quark state.

Results of a K-matrix approach [26] for πN and ηN final states provide realistic values for all considered partial widths, except for $\Gamma_{S_{11}(1650) \rightarrow \eta N}$.

Finally, in Ref. [7], studying the ηN final states, dispersion relations lead to values in agreement with data, while the isobar model tends to overestimate $\Gamma_{S_{11}(1535) \rightarrow \eta N}$.

The ambitious EBAC [79] program offers a powerful frame to study the properties of baryons, including partial decay widths [80], extraction of which requires non ambiguous determination of the poles positions [81]; a topic under extensive investigations [81–88].

2. Coupling constants $g_{S_{11}MB}$

In Table VI, predictions for the relevant resonance-meson-baryon coupling constants, $g_{S_{11}MB}$, from models A and B are given in particle basis.

In order to emphasize the most sensitive decay channels to the five-quark components in $S_{11}(1535)$, we compare results from models A and B. For $K^+\Sigma^0$ and $K^0\Sigma^+$, we observe variations by a factor of 2 between the two models, with central values differing from each other by more than 4σ . Next come $K^+\Lambda$ and ηp , with about 30% differences and 2σ . The other three channels ($\pi^0 p$, $\pi^+ n$, $\eta' p$) show no significant sensitivities to the five-quark components.

In the case of $S_{11}(1650)$, similar sensitivities are observed. However, the rather small

TABLE VI: S_{11} -meson-baryon coupling constants ($g_{S_{11}MB}$) in particle basis.

N^*	$\pi^0 p$	$\pi^+ n$	ηp	$K^+ \Lambda$	$K^0 \Sigma^+$	$K^+ \Sigma^0$	$\eta' p$	Ref.
$S_{11}(1535)$	-0.58 ± 0.13	0.82 ± 0.18	-2.57 ± 0.17	1.42 ± 0.11	0.95 ± 0.20	-0.62 ± 0.09	3.09 ± 0.20	Model A
	-0.63 ± 0.03	0.89 ± 0.04	-2.07 ± 0.15	1.76 ± 0.02	1.81 ± 0.06	-1.28 ± 0.04	3.33 ± 0.10	Model B
	± 0.39	± 0.56	± 1.84	± 0.92	± 2.12	± 1.50		[6]
$S_{11}(1650)$	-0.70 ± 0.10	0.94 ± 0.19	0.84 ± 0.40	0.67 ± 0.25	-1.42 ± 0.21	0.95 ± 0.10	-1.61 ± 0.79	Model A
	-0.94 ± 0.02	1.33 ± 0.03	0.35 ± 0.12	0.51 ± 0.03	-2.17 ± 0.05	1.53 ± 0.04	-1.62 ± 0.14	Model B

branching ratios to those final states, require substantial experimental efforts and sophisticated phenomenological approaches, e.g. for $\gamma p \rightarrow K^0 \Sigma^+$, $K^+ \Sigma^0$.

In Table VI, results from a chiral unitary approach [6] are also reported, showing compatible values with those of model B for $K^+ \Sigma^0$, $K^0 \Sigma^+$ and ηp . For the other three channels the two sets differ by roughly 60%.

 TABLE VII: S_{11} -meson-baryon coupling constants ($g_{S_{11}MB}$) in isospin basis.

N^*	πN	ηN	$K \Lambda$	$K \Sigma$	$\eta' N$	Approach	Ref.
$S_{11}(1535)$	-1.09 ± 0.05	-2.07 ± 0.15	1.76 ± 0.02	2.21 ± 0.07	3.3 ± 0.1	Model B	Present work
	$\pm(0.62 \pm 0.32)$	$\pm(0.97 \pm 0.45)$	$\pm(0.55 \pm 0.32)$	$\pm(0.55 \pm 0.32)$		PWA	Sarantsev <i>et al.</i> [24]
	± 0.6	± 2.1	± 1.7	± 2.4		Chiral Lagrangian	Gamermann <i>et al.</i> [30]
$S_{11}(1650)$	-1.64 ± 0.03	0.35 ± 0.14	0.53 ± 0.04	-2.66 ± 0.06	-1.62 ± 0.14	Model B	Present work
	$\pm(1.05 \pm 0.45)$	$\pm(0.63 \pm 0.32)$	$\pm(0.32 \pm 0.32)$	$\pm(0.71 \pm 0.39)$		PWA	Sarantsev <i>et al.</i> [24]
	± 1.2	± 0.8	± 0.6	± 1.7		Chiral Lagrangian	Gamermann <i>et al.</i> [30]

In Table VII, predictions in isospin basis are reported for model B and other sources. Additional results reported in the literature and limited to fewer channels are also discussed below.

Within an isobar approach [23], a combined analysis [24] of the pseudoscalar mesons photoproduction data available by 2005 has extracted coupling constants in isospin basis, with around $\pm 60\%$ uncertainties. The reported couplings $g_{S_{11}(1535)\pi N}$ and $g_{S_{11}(1535)\eta N}$ are compatible with the model B predictions within 2σ , while discrepancies between the two approaches for $g_{S_{11}(1535)K\Lambda}$ and $g_{S_{11}(1535)K\Sigma}$ reach factors 3 to 4 and 4σ . For the second resonance, results from the two calculations agree within 1σ for $g_{S_{11}(1650)\pi N}$, $g_{S_{11}(1650)\eta N}$ and $g_{S_{11}(1650)K\Lambda}$, with only significant disagreement observed for $g_{S_{11}(1650)K\Sigma}$. Copious data released since then, if interpreted within the same approach might bring in new insights into the coupling constants.

Results from a recent SU(6) extended chiral Lagrangian [30], embodying eleven meson-baryon final states, are also reported in Table VII and show consistent values between that approach and model B for $g_{S_{11}(1535)\eta N}$, $g_{S_{11}(1535)K\Lambda}$, $g_{S_{11}(1535)K\Sigma}$, and $g_{S_{11}(1650)K\Lambda}$.

An effective Lagrangian focused on interpreting [20] η production data in NN and πN collisions, leads to $g_{S_{11}(1535)\eta N} = 2.2$ and $g_{S_{11}(1650)\eta N} = 0.55$, compatible with our values. Another effective Lagrangian approach [18] studying η and η' production data in the same reactions gives $g_{S_{11}(1535)\eta' p} = 3.7$, about only 10% higher than the value given by model B.

Here, we wish to make a few comments with respect to the relative values of some of the coupling constants.

i) While the ηNN coupling constant is known to be smaller than that of πNN , the ratio $|g_{S_{11}(1535)\eta N}/g_{S_{11}(1535)\pi N}|$ comes out significantly larger than 1. This result is in line with the finding [43] that, in the soft pion limit, πNN^* coupling vanishes due to chiral symmetry, while that of ηNN^* remains finite.

ii) The ratio $|g_{S_{11}(1535)K\Lambda}/g_{S_{11}(1535)\eta N}|$ takes the value 1.3 ± 0.3 , within an isobar model [8] interpreting $J/\psi \rightarrow \bar{p}p\eta$ and $\psi \rightarrow \bar{p}K^+\Lambda$ data, larger than the results reported in Table VII. Dressed versus bare mass considerations [89], might affect the reported ratio in Ref. [8]. Investigation of the same reaction within a unitary chiral approach [6, 27] puts that ratio around 0.5 to 0.7, smaller than our result.

iii) The ratio $|g_{S_{11}(1650)K\Sigma}/g_{S_{11}(1650)K\Lambda}|$ turns out to be around 5. Actually, $S_{11}(1650)$ is dominant by the state $N(\frac{4}{3}P_M)_{\frac{1}{2}-}$, which cannot transit to $K\Lambda$ channel. Moreover, there is a cancellation between the contributions from $qqq \rightarrow K\Lambda$ and $qqqq\bar{q} \rightarrow K\Lambda$, which leads also to a very small decay width $\Gamma_{S_{11}(1650) \rightarrow K\Lambda}$. In addition, the threshold for $S_{11}(1650) \rightarrow K\Sigma$ decay channel being very close to the mass of $S_{11}(1650)$, contributions from the five-quark component enhance significantly the coupling constant $g_{S_{11}(1650)K\Sigma}$.

iv) It is worthy to be noticed that the coupling constants $g_{S_{11}\eta N}$, $g_{S_{11}K\Sigma}$ and $g_{S_{11}\eta' N}$ for $S_{11}(1535)$ and $S_{11}(1650)$ have opposite signs. Moreover, the ratio $|g_{S_{11}(1535)K\Sigma}/g_{S_{11}(1650)K\Sigma}|$ is close to unity. Those features might lead to significant cancellations in the interference terms in KY photo- and/or hadron-induced productions.

v) In Tables VI and VII, one finds the following orderings for magnitudes of the coupling constants, predicted by model B, and in Refs.[29, 30], noted below as **a)**, **b)** and **c)**, respectively:

- For $S_{11} \equiv S_{11}(1535)$:

- *In particle basis*

$$(a) : |g_{S_{11}\pi^0 p}| < |g_{S_{11}\pi^+ n}| < |g_{S_{11}K^+\Sigma^0}| < |g_{S_{11}K^+\Lambda}| \approx |g_{S_{11}K^0\Sigma^+}| < |g_{S_{11}\eta p}| < |g_{S_{11}\eta' p}| \quad (31)$$

$$(b) : |g_{S_{11}\pi^0 p}| \approx |g_{S_{11}K^+\Sigma^0}| < |g_{S_{11}\pi^+ n}| \approx |g_{S_{11}K^0\Sigma^+}| < |g_{S_{11}\eta p}| < |g_{S_{11}K^+\Lambda}|. \quad (32)$$

The main feature of our results **(a)** is that the strongest couplings are found the hidden strangeness sector, while those for open strangeness channels come out in between πN and ηN final states.

Inequalities in **(b)** come from a recent unitarized chiral effective Lagrangian [29], in which both $S_{11}(1535)$ and $S_{11}(1650)$ are dynamically generated. Within that model, the coupling to $K^+\Sigma^0$ is highly suppressed, and that to $K^+\Lambda$ turns out larger than coupling to ηp .

- *In isospin basis*

$$(a') : |g_{S_{11}\pi N}| < |g_{S_{11}K\Lambda}| < |g_{S_{11}\eta N}| \approx |g_{S_{11}K\Sigma}| < |g_{S_{11}\eta' N}|, \quad (33)$$

$$(c') : |g_{S_{11}\pi N}| < |g_{S_{11}K\Lambda}| < |g_{S_{11}\eta N}| \approx |g_{S_{11}K\Sigma}|. \quad (34)$$

Results from a chiral Lagrangian study [30], **(c')**, give the same ordering for couplings as model B. It is also the case for results from a chiral unitary approach [6], while another chiral unitary approach [44], distinguishing dynamically generated resonances from genuine quark states, leads to

$$|g_{S_{11}\pi N}| < |g_{S_{11}K\Lambda}| < |g_{S_{11}\eta N}| < |g_{S_{11}K\Sigma}|. \quad (35)$$

- **For $S_{11} \equiv S_{11}(1650)$:**

- *In particle basis*

$$(a) : |g_{S_{11}\eta p}| < |g_{S_{11}K^+\Lambda}| < |g_{S_{11}\pi^0 p}| < |g_{S_{11}\pi^+ n}| < |g_{S_{11}K^+\Sigma^0}| < |g_{S_{11}\eta' p}| < |g_{S_{11}K^0\Sigma^+}| \quad (36)$$

$$(b) : |g_{S_{11}K^+\Lambda}| < |g_{S_{11}\pi^0 p}| < |g_{S_{11}\pi^+ n}| \approx |g_{S_{11}K^+\Sigma^0}| < |g_{S_{11}\eta p}| < |g_{S_{11}K^0\Sigma^+}|. \quad (37)$$

In our model, the ordering in strangeness sector is separated by πN , according to the fact that the relevant disintegration channel is above or below the resonance mass.

The main differences between results from model B and those in Ref. [29] concern couplings to $K^+\Lambda$ and ηp .

- *In isospin basis*

$$(a') : |g_{S_{11}K\Lambda}| < |g_{S_{11}\eta N}| < |g_{S_{11}\pi N}| \approx |g_{S_{11}\eta' N}| < |g_{S_{11}K\Sigma}|, \quad (38)$$

$$(c') : |g_{S_{11}\eta N}| \lesssim |g_{S_{11}K\Lambda}| < |g_{S_{11}\pi N}| < |g_{S_{11}K\Sigma}|. \quad (39)$$

Here again model B and Ref. [30] lead basically to identical orderings.

To end this section, we would like to emphasize the following point, with respect to the importance of five-quark components. Our model leads to probability for the strangeness component in $S_{11}(1650)$ being smaller than that for the five-quark component in $S_{11}(1535)$. Moreover, the probability amplitude turns out to be positive for $S_{11}(1535)$, but negative for $S_{11}(1650)$.

Taking the ranges determined for probabilities (Eq. (30)), one gets $-77.4 \leq A_{5q}/A'_{5q} \leq -72.5$. This latter range and that for θ_S , embodied in Eq. (14), allow extracting values for the energy of the strangeness component, $1641.60 \leq E_5 \leq 1649.99$ MeV. The coupling between qqq and $qqqq\bar{q}$ in the corresponding baryon ${}_{5q}\langle\hat{V}_{cou}\rangle_{3q}$, Eq. (14), turns out to be negative for both S_{11} resonances.

3. Branching fraction versus branching ratio considerations

As mentioned earlier, in PDG [1] estimates for both branching fractions (BF) to meson-baryon states and branching ratios (BR), $(\Gamma_{MB}/\Gamma_{total})$, are reported. In the case of the S_{11} resonances considered here, those estimates are not identical for $S_{11}(1650) \rightarrow \eta N$, $K\Lambda$. In the present work we have used BR. However, a very recent work [46] has adopted BF. In order to compare the results of this latter work with those of model B, we have investigated the drawback of using BF instead of BR in our approach. Accordingly, a third model, hereafter called model C, was obtained.

Though we extract simultaneously the partial decay widths for both S_{11} resonances, the above changes in the data do not affect results for the $S_{11}(1535)$. In Table VIII, results from PDG, Ref. [46] and our models B and C are given for $S_{11}(1650)$. The $\chi^2_{d.p.}$ for the three models are comparable, namely, 0.15 (model B), 0.25 (model C) and 0.19 (ref. [46]).

Model C leads to results in agreement with the two other sets, within the uncertainties therein. Comparing models B and C, we observe that the most sensitive width is $\Gamma_{S_{11}(1650) \rightarrow K\Lambda}$ and to a lesser extent $\Gamma_{S_{11}(1650) \rightarrow \eta N}$, while $\Gamma_{S_{11}(1650) \rightarrow \pi N}$ increases very slightly.

In Table IX, results for coupling constant from models B and C are reported. We find of cours the same features as for partial decay widths. In addition, given the associated uncertainties, it turns out that $\Gamma_{S_{11}(1650) \rightarrow \eta' N}$ and $\Gamma_{S_{11}(1650) \rightarrow K\Sigma}$ change very slightly within the two models.

TABLE VIII: Strong decay widths (in MeV) for $S_{11}(1650)$.

Γ_{tot}	πN	ηN	$K\Lambda$	Approach	Ref.
165 ± 20	128 ± 29	3.8 ± 3.6	4.8 ± 0.7	BR	PDG [1]
	143 ± 5	4.5 ± 3.0	4.8 ± 0.7	Model B	Present work
	128 ± 29	10.7 ± 5.8	11.5 ± 6.6	BF	PDG [1]
	148 ± 8	9.7 ± 6.7	7.9 ± 0.3	Model C	Present work
	133 ± 33	12.5 ± 11.0	11.5 ± 6.4	$1/N_C$ -NLO	Jayalath <i>et al.</i> [46]

TABLE IX: $S_{11}(1650)$ -meson-baryon coupling constants ($g_{S_{11}MB}$) in isospin basis.

πN	ηN	$K\Lambda$	$K\Sigma$	$\eta' N$	Approach	Ref.
-1.64 ± 0.03	0.35 ± 0.14	0.53 ± 0.04	-2.66 ± 0.06	-1.62 ± 0.14	Model B	Present work
-1.66 ± 0.05	0.55 ± 0.16	0.62 ± 0.09	-2.49 ± 0.16	-1.74 ± 0.24	Model C	Present work

TABLE X: $S_{11}(1650)$ -meson-baryon coupling constants ($g_{S_{11}MB}$) in particle basis.

$\pi^0 p$	$\pi^+ n$	ηp	$K^+ \Lambda$	$K^0 \Sigma^+$	$K^+ \Sigma^0$	$\eta' p$	Ref.
-0.94 ± 0.02	1.33 ± 0.03	0.35 ± 0.14	0.51 ± 0.03	-2.17 ± 0.05	1.53 ± 0.04	-1.62 ± 0.14	Model B
-0.96 ± 0.03	1.36 ± 0.04	0.55 ± 0.16	0.62 ± 0.09	-2.03 ± 0.13	1.44 ± 0.09	-1.74 ± 0.24	Model C

Those trends are also present in the coupling constants given in particle basis (Table X).

Taking into account the associated uncertainties to the coupling constants, model C does not significantly modify the coupling constants ordering obtained in sec. III C 2 for model B.

To end this section, we give the phase space defined by model C:

$$24.7^\circ \leq \theta_S \leq 30.0^\circ ; 19.8\% \leq P_{5q} \leq 31\% ; 3.0\% \leq P'_{5q} \leq 12.6\% . \quad (40)$$

Compared to model B, Eq. (30), the ranges for θ_S and P_{5q} get slightly increased. The most significant change concerns P'_{5q} , which goes from $11\% \leq P'_{5q} \leq 18$ down to $3\% \leq P'_{5q} \leq 13$. This feature shows the sensitivity of $\Gamma_{S_{11}(1650) \rightarrow K\Lambda}$ and, to a lesser extent, that of $\Gamma_{S_{11}(1650) \rightarrow \eta N}$ to the five-quark components in $S_{11}(1650)$.

IV. SUMMARY AND CONCLUSIONS

Within a constituent quark approach, we studied the properties of four low-lying baryon resonances with respect to their partial decay widths to seven meson-baryon channels and associated resonance-meson-baryon coupling constants.

The starting point was the simplest chiral constituent quark model (χ CQM). The second step consisted in introducing $SU(6) \otimes O(3)$ breaking effects. Finally, five-quark components in the S_{11} resonances were implemented and investigated.

The outcome of the present work is reported below, focusing on the considered nucleon resonances ($S_{11}(1535)$, $S_{11}(1650)$, $D_{13}(1520)$ and $D_{13}(1700)$) and their strong decays to πN , ηN , $\eta' N$, $K\Lambda$ and $K\Sigma$ final states.

Within the χ CQM, the only adjustable parameter (ω_3) did not allow reproducing the partial widths of resonances. Introducing $SU(6) \otimes O(3)$ breaking, via configuration mixing angles θ_S and θ_D , brought in significant improvements with respect to the decay widths of the D_{13} resonances, but missed the data for the S_{11} resonances partial decay widths. Nevertheless, this second step allowed fixing the value of ω_3 and extracting ranges for the mixing angles, treated as free parameters. Trying to cure this unsatisfactory situation, possible roles due to five-quark component in the baryons' wave functions were investigated. Given that the latter issue is irrelevant with respect to the D_{13} resonances and the properties of which were well described in the second step, the final phase of our study was devoted to the S_{11} resonances.

We calculated the partial decay widths $S_{11}(1535) \rightarrow \pi N$, ηN and $S_{11}(1650) \rightarrow \pi$, ηN , $K\Lambda$ in the whole phase space defined by the mixing angle θ_S and the probability of five-quark components in each of the two resonances. Regions of the phase space allowing to reproduce the data for those widths were selected. Accordingly, that procedure allowed us extracting ranges for partial widths, with decay threshold below the relevant resonance mass, and resonance-meson-baryon coupling constants for the following meson-baryon combinations: $\pi^0 p$, $\pi^+ n$, ηp , $K^+ \Lambda$, $K^0 \Sigma^+$, $K^+ \Sigma^0$ and $\eta' p$.

The main findings of the present work are summarized below with respect to the approaches studied in describing the properties of the four low-lying nucleon resonances.

- The chiral constituent quark approach in three-quark configuration and exact $SU(6) \otimes O(3)$ symmetry is not appropriate to reproduce the known partial decay widths.

- Introducing symmetry breaking effects due to one-gluon-exchange mechanism, allows accounting for the partial decay width of the $D_{13}(1520)$ and $D_{13}(1700)$ resonances, but not for those of S_{11} resonances.
- Complementing the formalism with five-quark components in the S_{11} resonances leads to satisfactory results with respect to all known partial decay widths investigated here.
- The complete formalism puts ranges on the three adjustable parameters, namely, the mixing angle between configurations $|N_8^2 P_M\rangle$ and $|N_8^4 P_M\rangle$, and five-quark component probabilities in $S_{11}(1535)$ and $S_{11}(1650)$ resonances.
- For $S_{11}(1535)$, the most sensitive entities to the five-quark component turn out to be $\Gamma_{S_{11}(1535) \rightarrow \eta N}$, $g_{S_{11} K^+ \Sigma^0}$, $g_{S_{11} K^0 \Sigma^+}$ and $g_{S_{11} \eta p}$, all with sizeable magnitudes.
- For $S_{11}(1650)$, the same trends as for $S_{11}(1535)$ are observed. In addition $\Gamma_{S_{11}(1650) \rightarrow \pi N}$ undergoes significant change due to five-quark mixture. Here, ηN channel have smaller width and coupling constant compared to the $S_{11}(1535)$ case.

To go further, interpretation of recent data, obtained using electromagnetic and/or hadronic probes, within approaches with reasonable number of free parameters is very desirable. Within the present extended χ CQM approach, analysis of the $\gamma p \rightarrow \eta p$ data is underway [90].

Acknowledgments

One of us (C. S. A.) thanks X. H. Liu and J. J. Xie for very helpful discussions.

Appendix A: $S_{11}(1535)$ and $S_{11}(1650)$ resonances mixing angle in one-gluon-exchange and one-boson-exchange models

The mixing angle θ_S can be obtained by diagonalizing the following matrix:

$$\begin{pmatrix} \langle N(\frac{2}{8}P_M)_{\frac{1}{2}^-}, S_z | H_{hyp} | N(\frac{2}{8}P_M)_{\frac{1}{2}^-}, S_z \rangle, & \langle N(\frac{2}{8}P_M)_{\frac{1}{2}^-}, S_z | H_{hyp} | N(\frac{4}{8}P_M)_{\frac{1}{2}^-}, S_z \rangle \\ \langle N(\frac{4}{8}P_M)_{\frac{1}{2}^-}, S_z | H_{hyp} | N(\frac{2}{8}P_M)_{\frac{1}{2}^-}, S_z \rangle, & \langle N(\frac{4}{8}P_M)_{\frac{1}{2}^-}, S_z | H_{hyp} | N(\frac{4}{8}P_M)_{\frac{1}{2}^-}, S_z \rangle \end{pmatrix}, \quad (\text{A1})$$

where H_{hyp} is the hyperfine interaction between the quarks. In the OGE [58] and OBE models [59], the explicit forms of H_{hyp} are

$$H_{hyp}^{OGE} = \sum_{i < j} \frac{2\alpha_s}{3m_i m_j} \left\{ \frac{8\pi}{3} \vec{S}_i \cdot \vec{S}_j \delta^3(\vec{r}_{ij}) + \frac{1}{r_{ij}^3} \left[\frac{3\vec{S}_i \cdot \vec{r}_{ij} \vec{S}_j \cdot \vec{r}_{ij}}{r_{ij}^2} - \vec{S}_i \cdot \vec{S}_j \right] \right\} \quad (A2)$$

$$H_{hyp}^{OBE} = \sum_{i < j} \sum_F \frac{g^2}{4\pi} \frac{1}{12m_i m_j} \vec{\chi}_i^F \cdot \vec{\chi}_j^F \left\{ [\vec{\sigma}_i \cdot \vec{\sigma}_j \left(\frac{\mu^2 e^{-\mu r_{ij}}}{r_{ij}} - 4\pi \delta(\vec{r}_{ij}) \right)] \right. \\ \left. + \left(\frac{3\vec{\sigma}_i \cdot \vec{r}_{ij} \vec{\sigma}_j \cdot \vec{r}_{ij}}{r_{ij}^2} - \vec{\sigma}_i \cdot \vec{\sigma}_j \right) \frac{\mu^2 e^{-\mu r_{ij}}}{r_{ij}} \left(1 + \frac{3}{\mu r_{ij}} + \frac{3}{\mu^2 r_{ij}^2} \right) \right\} \quad (A3)$$

1. One-Gluon-Exchange (OGE) model

The OGE hyperfine interaction leads to the following matrix elements:

$$\langle N(\frac{2}{8}P_M)_{\frac{1}{2}^-, S_z} | H_{hyp}^{OGE} | N(\frac{2}{8}P_M)_{\frac{1}{2}^-, S_z} \rangle = -C, \quad (A4)$$

$$\langle N(\frac{2}{8}P_M)_{\frac{1}{2}^-, S_z} | H_{hyp}^{OGE} | N(\frac{2}{8}P_M)_{\frac{1}{2}^-, S_z} \rangle = C, \quad (A5)$$

$$\langle N(\frac{4}{8}P_M)_{\frac{1}{2}^-, S_z} | H_{hyp}^{OGE} | N(\frac{2}{8}P_M)_{\frac{1}{2}^-, S_z} \rangle = C, \quad (A6)$$

$$\langle N(\frac{4}{8}P_M)_{\frac{1}{2}^-, S_z} | H_{hyp}^{OGE} | N(\frac{4}{8}P_M)_{\frac{1}{2}^-, S_z} \rangle = 0, \quad (A7)$$

with the constant $C = \frac{2\alpha_s}{m^2} \omega_3^3 \pi^{-\frac{1}{2}}$, where m and ω_3 are the light quark mass and the harmonic oscillator parameter, respectively. Then, we obtain $\theta_S^{OGE} \simeq 32^\circ$.

Here a comment is in order with respect to the sign of θ_S . As, reported in Ref. [67], a non ambiguous entity with respect to that sign is the following ratio:

$$\mathcal{R} = \frac{\langle N | H_m | N(\frac{4}{8}P_M)_{\frac{1}{2}^-} \rangle}{\langle N | H_m | N(\frac{2}{8}P_M)_{\frac{1}{2}^-} \rangle}, \quad (A8)$$

with H_m the pseudovector couplings at the tree level. The ratio \mathcal{R} is a constant determined by $SU(6) \otimes O(3)$ symmetry.

Notice that in the present work, we have adopted the convention introduced by Koniuk and Isgur [31], where wave functions are in line with the $SU(3)$ conventions of de Swart [77]. In this frame, the constant \mathcal{R} gets a negative value, and the relevant mixing angle for the S -wave, θ_S , turns out positive. However, in line with the Hey, Litchfield, and Cashmore [91] analysis, Isgur and Karl in their early works [68, 70–72] used another convention, for which $\mathcal{R} = +1$ and $\theta_S < 0$. In the literature both conventions are being used, often without explicit mention of the utilized convention.

2. One-Boson-Exchange (OBE) model

The OBE hyperfine interaction results in

$$\langle N(\frac{2}{8}P_M)_{\frac{1}{2}^-, S_z} | H_{hyp}^{OBE} | N(\frac{2}{8}P_M)_{\frac{1}{2}^-, S_z} \rangle = 5V_{11} - 7V_{00}, \quad (\text{A9})$$

$$\langle N(\frac{2}{8}P_M)_{\frac{1}{2}^-, S_z} | H_{hyp}^{OBE} | N(\frac{2}{8}P_M)_{\frac{1}{2}^-, S_z} \rangle = -8T_{11}, \quad (\text{A10})$$

$$\langle N(\frac{4}{8}P_M)_{\frac{1}{2}^-, S_z} | H_{hyp}^{OBE} | N(\frac{2}{8}P_M)_{\frac{1}{2}^-, S_z} \rangle = -8T_{11}, \quad (\text{A11})$$

$$\langle N(\frac{4}{8}P_M)_{\frac{1}{2}^-, S_z} | H_{hyp}^{OBE} | N(\frac{4}{8}P_M)_{\frac{1}{2}^-, S_z} \rangle = 4V_{11} - 2V_{00} + 8T_{11}, \quad (\text{A12})$$

where V_{00} , V_{11} and T_{11} are constants from the orbital integral

$$V_{00} = \langle \varphi_{00} | \frac{g^2}{4\pi} \frac{1}{12m_i m_j} \left(\frac{\mu^2 e^{-\mu r_{ij}}}{r_{ij}} - 4\pi \delta(\vec{r}_{ij}) \right) | \varphi_{00} \rangle, \quad (\text{A13})$$

$$V_{11} = \langle \varphi_{1m} | \frac{g^2}{4\pi} \frac{1}{12m_i m_j} \left(\frac{\mu^2 e^{-\mu r_{ij}}}{r_{ij}} - 4\pi \delta(\vec{r}_{ij}) \right) | \varphi_{1m} \rangle, \quad (\text{A14})$$

$$T_{11} = \langle \varphi_{1m} | \frac{g^2}{4\pi} \frac{1}{12m_i m_j} \frac{\mu^2 e^{-\mu r_{ij}}}{r_{ij}} \left(1 + \frac{3}{\mu r_{ij}} + \frac{3}{\mu^2 r_{ij}^2} \right) | \varphi_{1m} \rangle. \quad (\text{A15})$$

Taking the same values for the parameters as in Ref. [59], we obtain $\theta_S = -13^\circ$. However, if one considers contributions from the vector meson exchanges, the absolute value of θ_S might be decreased, or even the sign might change [74, 76].

Relevance of the OGE versus the OBE has been studied by several authors, see e.g. Refs. [36, 40, 92, 93], favoring OGE mechanism, endorsed by the present work, as the origin of the $SU(6) \otimes O(3)$ symmetry breakdown.

-
- [1] K. Nakamura *et al.* [Particle Data Group], J. Phys. G **37**, 075021 (2010).
 - [2] N. Kaiser, P. B. Siegel and W. Weise, Phys. Lett. B **362**, 23 (1995).
 - [3] D. O. Riska and G. E. Brown, Nucl. Phys. A **679**, 577 (2001).
 - [4] G. Penner and U. Mosel, Phys. Rev. C **66**, 055211 (2002).
 - [5] G. Penner and U. Mosel, Phys. Rev. C **66**, 055212 (2002).
 - [6] T. Inoue, E. Oset and M. J. Vicente Vacas, Phys. Rev. C **65**, 035204 (2002).
 - [7] I. G. Aznauryan, Phys. Rev. C **68**, 065204 (2003).
 - [8] B. C. Liu and B. S. Zou, Phys. Rev. Lett. **96**, 042002 (2006).
 - [9] W. T. H. Chiang, F. Tabakin, T. S. H. Lee and B. Saghai, Phys. Lett. B **517**, 101 (2001).

- [10] W. T. Chiang, B. Saghai, F. Tabakin and T. S. H. Lee, Phys. Rev. C **69**, 065208 (2004).
- [11] K. Nakayama and H. Haberzettl, Phys. Rev. C **69**, 065212 (2004).
- [12] K. Nakayama and H. Haberzettl, Phys. Rev. **C73**, 045211 (2006).
- [13] K. Nakayama, Y. Oh and H. Haberzettl, arXiv:0803.3169 [hep-ph].
- [14] T. P. Vrana, S. A. Dytman and T. S. H. Lee, Phys. Rept. **328**, 181 (2000).
- [15] A. Matsuyama, T. Sato and T. S. Lee, Phys. Rept. **439**, 193 (2007).
- [16] B. Julia-Diaz, T. S. Lee, A. Matsuyama and T. Sato, Phys. Rev. C **76**, 065201 (2007).
- [17] J. Durand, B. Julia-Diaz, T. S. Lee, B. Saghai and T. Sato, Phys. Rev. C **78**, 025204 (2008).
- [18] X. Cao and X. G. Lee, Phys. Rev. C **78**, 035207 (2008).
- [19] R. Shyam, H. Lenske and U. Mosel, Phys. Rev. C **69**, 065205 (2004).
- [20] R. Shyam, Phys. Rev. C **75**, 055201 (2007).
- [21] V. Shklyar, H. Lenske and U. Mosel, Phys. Lett. B **650**, 172 (2007).
- [22] R. A. Arndt, W. J. Briscoe, T. W. Morrison, I. I. Strakovsky, R. L. Workman and A. B. Gridnev, Phys. Rev. C **72**, 045202 (2005).
- [23] A. V. Anisovich, A. Sarantsev, O. Bartholomy, E. Klempt, V. A. Nikonov and U. Thoma, Eur. Phys. J. A **25**, 427 (2005).
- [24] A. V. Sarantsev, V. A. Nikonov, A. V. Anisovich, E. Klempt and U. Thoma, Eur. Phys. J. A **25**, 441 (2005).
- [25] L. P. Kaptari and B. Kampfer, Eur. Phys. J. **A37**, 69-80 (2008).
- [26] S. Ceci, A. Svarc, B. Zauner, M. Manley and S. Capstick, Phys. Lett. B **659**, 228 (2008).
- [27] L. S. Geng, E. Oset, B. S. Zou and M. Doring, Phys. Rev. C **79**, 025203 (2009).
- [28] J. J. Xie and C. Wilkin, Phys. Rev. C **82**, 025210 (2010).
- [29] P. C. Bruns, M. Mai and U. G. Meissner, Phys. Lett. B **697**, 254 (2011).
- [30] D. Gamermann, C. Garcia-Recio, J. Nieves and L. L. Salcedo, arXiv:1104.2737 [hep-ph].
- [31] R. Koniuk and N. Isgur, Phys. Rev. D **21**, 1868 (1980) [Erratum-ibid. D **23**, 818 (1981)].
- [32] S. Capstick and W. Roberts, Phys. Rev. D **47**, 1994 (1993).
- [33] S. Capstick and W. Roberts, Phys. Rev. D **49**, 4570 (1994).
- [34] S. Capstick and W. Roberts, Phys. Rev. D **58**, 074011 (1998).
- [35] S. Capstick and W. Roberts, Prog. Part. Nucl. Phys. **45**, S241 (2000).
- [36] S. Capstick and W. Roberts, Fizika B **13**, 271 (2004).
- [37] A. Kiswandhi, S. Capstick and S. Dytman, Phys. Rev. C **69**, 025205 (2004).

- [38] B. Golli and S. Sirca, Eur. Phys. J. A **47**, 61 (2011).
- [39] H. c. Kim and S. H. Lee, Phys. Rev. D **56**, 4278 (1997).
- [40] T. Yoshimoto, T. Sato, M. Arima and T. S. H. Lee, Phys. Rev. C **61**, 065203 (2000).
- [41] S. L. Zhu, Mod. Phys. Lett. A **13**, 2763 (1998).
- [42] S. L. Zhu, W. Y. P. Hwang and Y. B. P. Dai, Phys. Rev. C **59**, 442 (1999).
- [43] D. Jido, M. Oka and A. Hosaka, Phys. Rev. Lett. **80**, 448 (1998).
- [44] T. Hyodo, D. Jido and A. Hosaka, Phys. Rev. C **78**, 025203 (2008).
- [45] J. L. Goity and N. N. Scoccola, Phys. Rev. D **72**, 034024 (2005).
- [46] C. Jayalath, J. L. Goity, E. G. de Urreta and N. N. Scoccola, arXiv:1108.2042 [nucl-th].
- [47] Q. B. Li and D. O. Riska, Phys. Rev. C **73**, 035201 (2006).
- [48] B. Julia-Diaz and D. O. Riska, Nucl. Phys. A **780**, 175 (2006).
- [49] C. S. An, D. O. Riska and B. S. Zou Phys. Rev. C **73**, 035207 (2006).
- [50] Q. B. Li and D. O. Riska, Phys. Rev. C **74**, 015202 (2006).
- [51] Q. B. Li and D. O. Riska, Nucl. Phys. A **766**, 172 (2006).
- [52] C. S. An and B. S. Zou, Eur. Phys. J. A **39**, 195 (2009).
- [53] C. S. An and D. O. Riska, Eur. Phys. J. A **37**, 263 (2008).
- [54] C. S. An, B. Saghai, S. G. Yuan and J. He, Phys. Rev. C **81**, 045203 (2010).
- [55] B. S. Zou, Nucl. Phys. A **827**, 333C (2009).
- [56] B. S. Zou, Nucl. Phys. A **835**, 199 (2010).
- [57] D. O. Riska, Chin. Phys. C **34**, 9 (2010).
- [58] A. De Rujula, H. Georgi and S. L. Glashow, Phys. Rev. D **12**, 147 (1975).
- [59] L. Y. Glozman and D. O. Riska, Phys. Rept. **268**, 263 (1996).
- [60] Q. B. Li and D. O. Riska, Nucl. Phys. A **791**, 406 (2007).
- [61] J. L. Goity and W. Roberts, Phys. Rev. D **60**, 034001 (1999).
- [62] T. A. Lahde and D. O. Riska, Nucl. Phys. A **710**, 99 (2002).
- [63] C. Gobbi, F. Iachello and D. Kusnezov, Phys. Rev. D **50**, 2048 (1994).
- [64] W. Rarita and J. Schwinger, Phys. Rev. **60**, 61 (1941).
- [65] L. M. Nath, B. Etemadi and J. D. Kimel, Phys. Rev. D **3**, 2153 (1971).
- [66] T.E.O. Ericson and W. Weise, *Pions and Nuclei* (Clarendon, Oxford, 1988).
- [67] B. Saghai and Z. Li, Few Body Syst. **47**, 105 (2010).
- [68] N. Isgur and G. Karl, Phys. Lett. B **72**, 109 (1977).

- [69] N. Isgur, G. Karl and R. Koniuk, Phys. Rev. Lett. **41**, 1269 (1978) [Erratum-ibid. **45**, 1738 (1980)].
- [70] N. Isgur and G. Karl, Phys. Lett. B **74**, 353 (1978).
- [71] N. Isgur and G. Karl, Phys. Rev. D **18**, 4187 (1978).
- [72] N. Isgur and G. Karl, Phys. Rev. D **19**, 2653 (1979) [Erratum-ibid. D **23**, 817 (1981)].
- [73] N. Isgur, Phys. Rev. D **62**, 054026 (2000).
- [74] L. Y. Glozman, arXiv:nucl-th/9909021.
- [75] J. Chizma and G. Karl, Phys. Rev. D **68**, 054007 (2003).
- [76] L. Y. Glozman, Surveys High Energ. Phys. **14**, 109 (1999).
- [77] J. J. de Swart, Rev. Mod. Phys. **35**, 916 (1963) [Erratum-ibid. **37**, 326 (1965)].
- [78] C. An and B. Saghai, arXiv:1107.5991 [nucl-th].
- [79] Excited Baryon Analysis Center: <http://ebac-theory.jlab.org/>.
- [80] H. Kamano, B. Julia-Diaz, T. -S. H. Lee, A. Matsuyama and T. Sato, Phys. Rev. **C79**, 025206 (2009).
- [81] N. Suzuki, T. Sato and T. -S. H. Lee, Phys. Rev. **C79**, 025205 (2009).
- [82] S. Capstick *et al.*, Eur. Phys. J. A **35**, 253 (2008).
- [83] M. Doring, C. Hanhart, F. Huang, S. Krewald and U. G. Meissner, Phys. Lett. B **681**, 26 (2009).
- [84] M. Doring, C. Hanhart, F. Huang, S. Krewald and U. G. Meissner, Nucl. Phys. A **829**, 170 (2009).
- [85] M. Doring and K. Nakayama, Eur. Phys. J. A **43**, 83 (2010).
- [86] E. Oset and A. Ramos, Eur. Phys. J. A **44**, 445 (2010).
- [87] S. Ceci, M. Doring, C. Hanhart, S. Krewald, U. G. Meissner and A. Svarc, Phys. Rev. C **84**, 015205 (2011).
- [88] H. Osmanovic, S. Ceci, A. Svarc, M. Hadzimehmedovic and J. Stahov, arXiv:1103.2855 [hep-ph].
- [89] S. Ceci, A. Svarc and B. Zauner, Phys. Rev. Lett. **102**, 209101 (2009).
- [90] C. S. An, J. He and B. Saghai, *in progress*.
- [91] A. J. G. Hey, P. J. Litchfield and R. J. Cashmore, Nucl. Phys. B **95**, 516 (1975).
- [92] J. He and Y. -B. Dong, Nucl. Phys. **A725**, 201-210 (2003).
- [93] J. Liu, J. He and Y. B. Dong, Phys. Rev. **D71**, 094004 (2005).